ISSN 0006-2979, Biochemistry (Moscow), 2016, Vol. 81, No. 2, pp. 122-134. © Pleiades Publishing, Ltd., 2016.
Published in Russian in Biokhimiya, 2016, Vol. 81, No. 2, pp. 215-230.
Originally published in Biochemistry (Moscow) On-Line Papers in Press, as Manuscript BM15-282, December 27, 2015.

Structure, Chaperone Activity, and Aggregation of Wild-Type and R12C Mutant αB-Crystallins in the Presence of Thermal Stress and Calcium Ion – Implications for Role of Calcium in Cataract Pathogenesis

M. Ragerdi Kashani[1], R. Yousefi[1]*, M. Akbarian[1], M. M. Alavianmehr[2], and Y. Ghasemi[3]

[1]*Shiraz University, Protein Chemistry Laboratory (PCL), Department of Biology, 71345 Shiraz, Iran; fax: + (98) 711-32280916; E-mail: ryousefi@shirazu.ac.ir*
[2]*Shiraz University of Technology, Department of Chemistry, Shiraz, Iran*
[3]*Department of Pharmaceutical Biotechnology and Pharmaceutical Sciences Research Center, School of Pharmacy, Shiraz University of Medical Sciences, Shiraz, Iran*

Received August 9, 2015
Revision received September 19, 2015

Abstract—The current study was performed with the aim to evaluate the chaperoning ability, structural features, and aggregation propensity of wild-type and R12C mutant αB-crystallins (αB-Cry) under thermal stress and in the presence of calcium ion. The results of different spectroscopic analyses suggest that wild-type and mutant αB-Cry have dissimilar secondary and tertiary structures. Moreover, αB-Cry indicates slightly improved chaperone activity upon the R12C mutation. Thermal stress and calcium, respectively, enhance and reduce the extent of solvent-exposed hydrophobic surfaces accompanying formation of ordered and non-ordered aggregate entities in both proteins. Compared to the wild-type protein, the R12C mutant counterpart shows significant resistance against thermal and calcium-induced aggregation. In addition, in the presence of calcium, significant structural variation was accompanied by reduction in the solvent-exposed hydrophobic patches and attenuation of chaperone activity in both proteins. Additionally, gel mobility shift assay indicates the intrinsic propensity of R12C mutant αB-Cry for disulfide bridge-mediated protein dimerization. Overall, the results of this study are of high significance for understanding the molecular details of different factors that are involved in the pathomechanism of cataract disorders.

DOI: 10.1134/S0006297916020061

Key words: αB-crystallin, R12C mutation, chaperone, thermal stress, aggregation

As a member of small heat shock protein family (sHsps), α-crystallin (α-Cry) prevents precipitation and aggregation of partially unfolded proteins in lenticular tissues, maintaining transparency of the eye lens throughout the lifespan [1]. This chaperone comprises up to 40% of total soluble lens proteins and is made up of αA- (173 residues) and αB-Cry (175 residues) in a 3 : 1 ratio [2, 3]. In addition to the lenticular tissues, αA- and αB-Cry are expressed in other tissues; for instance, αB-Cry is significantly expressed in tissues such as heart, muscle, kidney, and brain, and trace expression of αA-Cry has been detected in spleen and thymus [4]. Numerous studies have noted the development of age-related cataract due to the reduction in chaperone activity of α-Cry [5, 6]. Both mutations in α-Cry genes and accumulation of posttranslational modifications are known as the major causes for deteriorating protein chaperone activity during aging [7]. Moreover, upregulation of αB-Cry has been already reported in pathological states such as ischemic heart, multiple sclerosis, Alzheimer's, Parkinson's, and Alexander's diseases [8]. Additionally, αB-Cry has been recently considered as a significant therapeutic target, particularly in cancer pathology [9]. The quaternary structure of αB-Cry is sensitive to environmental factors such as pH, temperature, ionic strength, and calcium ions, which alter the oligomeric assembly, domain dynamics, and intrinsic subunit exchange; accordingly, all of these environmental and molecular events are critical for chaperone activity of this protein [10, 11].

* To whom correspondence should be addressed.

As reported earlier, bivalent metal ions such as calcium have significant impact on both structure and chaperone activity of α-Cry [4, 10]. Additionally, the induction of αB-Cry by bivalent metal ions has been reported [8]. In addition, calcium has long been known to play a role in cataract development, and its concentration in cataractous lenses ranged from 0.1 to 64 mM [12]. The intracellular calcium/sodium levels in the lens of 70% of human cataracts are dramatically elevated [13]. The calcium concentration in the lens cytoplasm is 100-1000 times lower than its level in the surrounding aqueous humor; accordingly, permeability of this metal ion occurs by passive transport through calcium channels and diffusion across the lipid bilayer [13]. On the other hand, calcium pumps, by extruding calcium out of the cell, play an essential function for maintaining low physiological levels of intracellular calcium [14]. Under pathological conditions such as diabetes and during aging, membrane defects lead to significant reduction in calcium ATPase activity and increase calcium inward leak (scheme).

The eye lens consists of a layer of epithelial cells, overlaying a series of differentiating fiber cells, which upon maturation lose their organelles [13]. Therefore, the alteration in plasma membrane of lens fiber cells may have important consequences on their cytoplasmic calcium levels. The cytoplasmic accumulation of lenticular calcium to pathological levels produces lens opacity and light scattering in a number of ways. For instance, high level of cytoplasmic calcium, as indicated in the scheme, results in activation of calpain, which subsequently participates in the hydrolysis of lens crystallin, leading to development of lens opacification [15]. Additionally, calcium reduces chaperone defense ability of α-Cry, which is important to prevent aggregation of other proteins in lenticular tissues [5, 16]. In addition, this bivalent metal ion induces aggregation of lens crystallin, and its prolonged elevation in cytoplasm results in increased production of reactive oxygen species (ROS), which can subsequently modify lens proteins [17]. Overall, all of the calcium-induced changes mentioned above are known as important contributory factors in development of lens opacity and cataract diseases. Arginine 12 (R12) is a conserved residue in αB- and αA-Crys, as well as in Hsp27. The R12C mutation in the αA-Cry gene has been reported to be associated with development of congenital cataract [18]. The objective in the current study was to compare structure, chaperone activity, and aggregation propensity of wild-type and R12C mutant αB-Cry in the presence of calcium ion.

MATERIALS AND METHODS

Sephacryl S-300 HR, Q-Sepharose anion-exchange column, thioflavin T (ThT), 1-anilino-8-naphthalene sulfonate (ANS), bovine pancreatic insulin, isopropyl β-

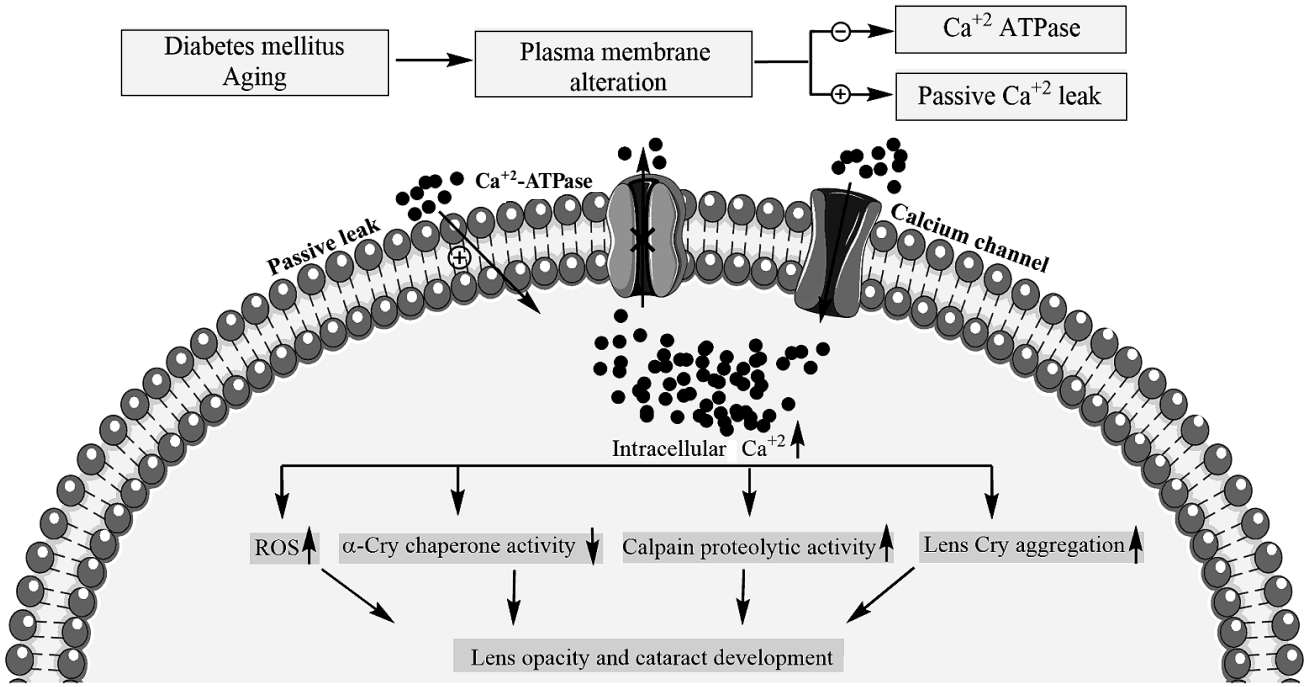

Effect of diabetes and aging on intracellular calcium level and downstream pathological consequences in lenticular tissues. The biochemical pathways leading to pathological elevation of lenticular calcium levels are indicated in diabetes and during aging. In addition, the downstream pathomechanisms that are involved in calcium-induced lens opacification and cataract development are shown

Scheme

D-thiogalactopyranoside (IPTG), $CaCl_2$, and other chemicals were purchased from Sigma Chemical Company (USA).

Cloning and purification of wild-type and mutant αB-Cry. Site directed mutagenesis was generated using the QuikChange Lightning Multi Site-Directed Mutagenesis Kit. The cDNA of human αB-Cry was constructed in pET-28b(+) expression vector. To construct αB mutant, Arg12 was replaced by Cys (R12C), and the resulting PCR product was digested with methylation sensitive restriction enzyme DpnI and then transformed into *E. coli* XL10-Gold cells. A mutant plasmid from the resulting colonies was sequenced to confirm the mutation occurred. For expression and purification of the recombinant proteins, plasmid of human wild-type and mutant αB-Cry were transformed into *E. coli* BL21(DE3) [19]. Then the transformants were grown in Luria broth (LB) medium containing kanamycin (50 μg/ml) at 37°C. When the optical density at 600 nm reached ~0.6, expression was induced by addition of IPTG (250 μM) to the LB medium, and the incubation was continued for another 12 h at 37°C. Cell pellet was obtained by centrifugation of the LB medium at 6000 rpm for 20 min, and it was resuspended in lysis buffer A (25 mM Tris (pH 8.0), 100 mM NaCl, 0.5 mM EDTA, 10 mM β-mercaptoethanol (β-ME), and 0.01% NaN_3) at a ratio of 3 ml of buffer to 1 g (w/w) of cells. The cells in the suspension were lysed by sonication, and the bacterial lysate was centrifuged at 8000 rpm for 40 min at 4°C. The resulting supernatant was applied onto a Q-Sepharose anion-exchange column that was equilibrated with buffer B (25 mM Tris, 0.5 mM EDTA, 10 mM β-ME, and 0.01% NaN_3 with pH 7.2) [20-22]. The flow rate was fixed at 1 ml/min in the presence of a 0-0.5 M NaCl gradient. Purity was assessed by SDS-PAGE, and the highly pure fractions were collected and dialyzed overnight against buffer A at 4°C. The concentrated protein sample was then applied onto a Sephacryl S-300 HR (100 × 1.5 cm) gel filtration column that had been pre-equilibrated with the same buffer at 4°C [23, 24]. Protein fractions were taken with a flow rate and fraction size of 0.25 ml/min and 2 ml, respectively. As purity of human αB-Cry was judged on SDS-PAGE (gel 12%), the highly purified fractions were collected and dialyzed against distilled water. Then the purified protein was lyophilized and stored at −20°C. In addition, lens γ-Cry was purified according to a previously published protocol [25]. In brief, bovine lenses were obtained from a local slaughterhouse and dissected from the eyeballs. Then lens homogenate (10% w/v) was prepared in buffer A and centrifuged at 14,000 rpm for 30 min at 4°C. The supernatant of total soluble lens proteins (TSPs) was collected and applied on a Sephacryl S-300 HR (100 × 1.5 cm) gel filtration column that was pre-equilibrated with the same buffer at 4°C [26]. The flow rate and fraction size were adjusted to 0.25 ml/min and 2 ml, respectively, and purity of γ-Cry was assessed on SDS-PAGE. At the end, highly pure fractions were collected, lyophilized, and stored at −20°C until use.

Fluorescence measurements. Fluorescence was measured using a Cary-100 fluorescence instrument (Varian, Australia) equipped with a Peltier temperature control unit. The fluorescence measurements were performed to compare the impact of calcium and thermal stress (incubation for 2 h at 60°C) on structure and amyloidogenic properties of wild-type and mutant αB-Cry. Fluorescence was measured at 25°C in 50 mM Tris buffer, pH 7.2, containing 100 mM NaCl (buffer C). The Trp fluorescence spectra of αB-Cry (0.15 mg/ml) were recorded with excitation wavelength 295 nm, and the emission spectra were determined in the 300-500-nm range [24, 27]. In addition, the surface hydrophobicity of αB-Cry was studied using the fluorescence probe ANS (emission 400-600 nm, excitation 365 nm) [24, 28]. Prior to the measurements, αB-Cry (0.15 mg/ml) was incubated for 30 min with ANS (100 μM) at room temperature. Moreover, the amyloidogenic activity of these recombinant proteins was assessed in the presence of fluorescence probe ThT [28]. Prior to the measurements, αB-Cry (0.15 mg/ml) was incubated with 20 μM ThT for 5 min. Then, the fluorescence spectra were taken between 450-600 nm with excitation wavelength at 440 nm.

CD assessment. The far UV-CD spectra (190-260 nm, 25°C) were recorded on a CD spectrophotometer instrument (Model-215; Aviv, USA). The CD spectra of αB-Cry (0.2 mg/ml) were collected in the wavelength range 190-260 nm using a cylindrical quartz cell of 1-mm path length [24]. The results are expressed as mean residue ellipticity at wavelength λ, $[\theta]_{mrw,\lambda}$ ($deg \cdot cm^2 \cdot dmol^{-1}$), which is given by the following equation:

$$[\theta]_{mrw,\lambda} = MRW \times \theta_\lambda / 10 \times d \times c, \quad (1)$$

where MRW stands for the mean residue weight of the peptide bond, θ_λ is the observed ellipticity (degrees) at wavelength λ, d is the pathlength (cm), and c is the protein concentration (g/ml) with 115 Da as residue molecular weight [29, 30]. Also, $MRW = M/(N-1)$, where M is the molecular mass of the polypeptide chain (Da) and N is the number of amino acids in the chain. The spectrum of buffer C without protein was subtracted from each recorded spectrum. The secondary structure content of αB-Cry was calculated with the CDNN CD spectra deconvolution software [24, 31].

Aggregation propensity of wild-type and mutant αB-Crys. For this study, the aggregation propensity of wild-type and mutant αB-Cry was evaluated in the presence of calcium ion and under thermal stress. The αB-Cry (1 mg/ml) was incubated in buffer C with different concentrations of calcium ion at 37°C for one week. In addition, the recombinant proteins were incubated under thermal stress at 60°C for 2 h in buffer C. At the end of the

incubation, the protein samples were diluted to final concentration 0.5 mg/ml, and absorption spectra were collected in the wavelength range 200-700 nm [32]. In addition, protein aggregation was evaluated in a kinetic fashion in the presence of calcium and under thermal stress.

Chaperone activity measurements. The chaperone activity of wild-type and mutant αB-Cry was evaluated under both chemical and thermal stresses in buffer C. Insulin (0.3 mg/ml) and γ-Cry (0.3 mg/ml) were used as the target proteins in the chemical and thermally induced aggregation systems, respectively. While aggregation of insulin was initiated by 20 mM dithiothreitol (DTT) at 40°C, that of γ-Cry was induced at 60°C [19]. The aggregation of target proteins was monitored by following the absorption increment at 360 nm on a T90$^+$ UV-Vis spectrophotometer instrument (PG Instrument Ltd, UK) equipped with a Peltier temperature controller (PCT-2 model). In addition, the impact of calcium was evaluated on the chaperone activity of αB-Cry in both systems.

SDS-PAGE analysis. The SDS-PAGE experiments were done on 12% gel using the standard Laemmli protocol. After electrophoresis, the protein bands were visualized using the Coomassie brilliant blue (CBB) staining method [24, 33].

Protein assay. The concentration of bovine pancreatic insulin, human αB-Cry, and bovine lens γ-Cry were determined using their corresponding molar absorption coefficients [24, 27]. In addition, the concentration of crude lens protein sample was determined using a standard Bradford protocol [26, 27].

RESULTS AND DISCUSSION

Importance of Arg-to-Cys mutation in α-Cry. The Arg-to-Cys mutation is of high importance because the positive charge and long side chain of Arg is converted to a polar and non-charged residue in Cys. Moreover, the incorporation of an additional Cys residue may have pathological consequence because Cys has ability to form both inter- and intramolecular disulfide bonds, which has been already shown to contribute in the pathogenesis of cataract disorders [34, 35]. In addition, a disulfide cross-link has already been shown to alter the mass of α-Cry oligomers. Therefore, the size distribution of this protein is highly significant in both protein chaperone activity and the ability of lens to refract or focus light sharply on the retina. As reported, Arg12 is a conserved residue amongst sHSPs, particularly in HSP27, αA-Cry, and αB-Cry. The R12C mutation in αA-Cry has been shown to cause a congenital cataract disorder [36, 37]. Accordingly, we sought to determine if this mutation could cause any change in structure, aggregation, and functional properties of αB-Cry, as this protein has wide distribution in various tissues in addition to the ocular system. To express the recombinant proteins, plasmid of human wild-type and mutant αB-Cry was transformed into *E. coli* BL21(DE3).

After successful expression, the protein was purified using sequential chromatographic methods (anion-exchange and gel-filtration chromatography). Then, the purification quality was judged using SDS-PAGE analysis. As shown in Fig. 1, the pure sample of both wild-type (lane *3*) and R12C αB-Cry (lane *4*) were used for further studies. Additionally, γ-Cry from bovine lens was purified by gel filtration chromatography (lane *5*) and used as a client protein for the assessment of chaperone activity of the recombinant αB-Crys in a thermally induced aggregation system.

Structural characterization of wild-type and mutant R12C αB-Cry. The fluorescence of Trp along with far UV-CD was used to determine possible changes in tertiary and secondary structure of αB-Cry after the R12C mutation. As shown in Fig. 2a, the mutant αB-Cry has significantly lower Trp fluorescence intensity than wild-type protein counterpart does. This result suggests that the Trp residue in R12C αB-Cry is located in a polar environment, and the two proteins have dissimilar tertiary structures. These results are in contrast to those reported for the R12A mutation [18]. This contradiction can be explained with the specific impact of the newly incorpo-

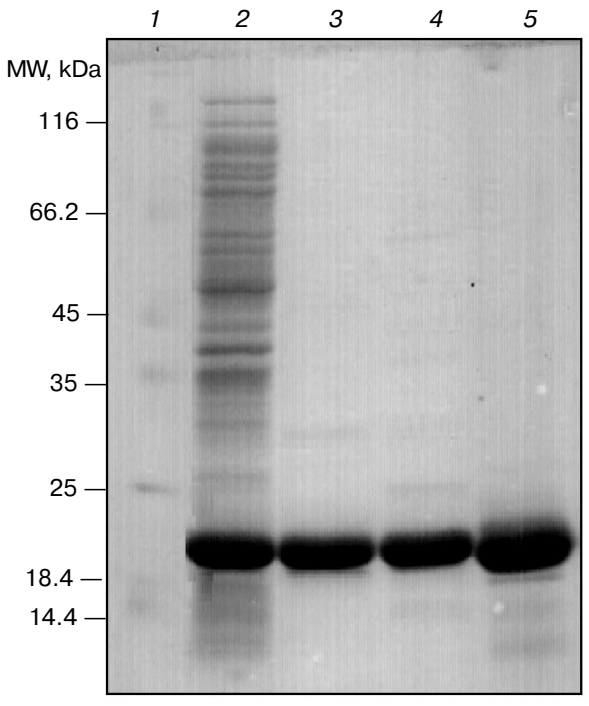

Fig. 1. SDS-PAGE analysis of purified Cry samples. An aliquot (12 μg) of each protein sample was taken and subjected to SDS-PAGE analysis (12% gel), under reducing condition. The protein bands were visualized by an appropriate CBB staining procedure. Lanes *1-5*, respectively, stand for molecular mass markers, crude protein sample, wild-type αB-Cry, R12C mutant αB-Cry, and γ-Cry.

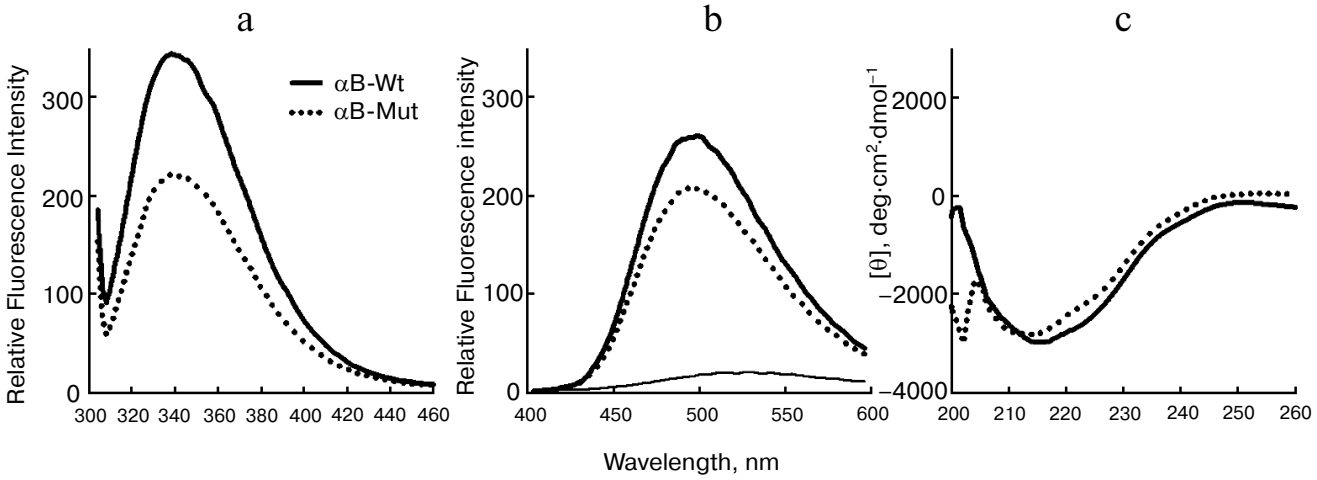

Fig. 2. Structural analysis of wild-type and R12C mutant αB-Crys. a) Trp fluorescence emission spectra of the recombinant proteins at concentration 0.15 mg/ml were recorded between 300-500 nm at 25°C with excitation wavelength 295 nm. b) Protein surface hydrophobicity was investigated with ANS fluorescence measurements, as each protein sample (0.15 mg/ml) was incubated individually with ANS (100 μM) for 30 min at 25°C. The samples were excited at 365 nm, and the emission spectra were recorded in the range 400-600 nm. c) Far UV-CD spectra of these proteins at concentration 0.2 mg/ml recorded at room temperature with cell pathlength 0.1 mm. The experiments were done in 50 mM Tris buffer, pH 7.2, containing 100 mM NaCl (buffer C).

rated Cys residue on the structure of αB-Cry. The solvent-exposed hydrophobic patches play a significant role in chaperone activity of α-Cry [34].

Accordingly, ANS fluorescence was studied to compare these two recombinant proteins in the terms of their exposed hydrophobic surfaces. As indicated in Fig. 2b, the R12C mutant protein shows lower ANS fluorescence intensity than wild-type protein counterpart, suggesting that this mutation can reduce the solvent exposed hydrophobic patches of the mutant protein. In fact, the wild-type protein displays more solvent exposed hydrophobic surfaces than the mutant protein counterpart does. Far UV-CD analysis indicates that these two proteins have different secondary structural contents (Fig. 2c). Quantitative analysis of the far UV-CD data using the CDNN CD spectra deconvolution software showed that the majority of secondary structures of these proteins were β-sheet (table). Moreover, because of the R12C mutation, an increment in α-helix/random coil contents with reduction in the percentage of β-sheet structure was observed (table). Overall, the R12C mutation results in both secondary and tertiary structural alteration of αB-Cry.

Chaperone activity of wild-type and mutant R12C αB-Cry. It is believed that lens opacification and cataract formation are the results of loss of chaperone efficiency of α-Cry, which can be due to either gene mutation or accumulation of various posttranslational modifications of this protein [7]. The chaperone activity is quantified by estimation of three different parameters including A_{lim} (the limiting value of absorbance at $t \rightarrow \infty$), the product $k_I A_{lim}$ (the initial rate of aggregation, where k_I is the rate constant of the first order [38]), and t_{onset} (the lag time before initiation of aggregation). For quantification of chaperone activity, these parametes can be used either alone or in combination [39].

The following equation can be used to express the chaperone activity in terms of percentage of protection with the use of the three important parameters mentioned above:

$$\% \text{ protection} = (1 - Ar/Ar_0) \times 100. \quad (2)$$

In this equation, Ar and Ar_0 are the areas under the curves of optical density versus time in the presence and absence of the chaperone, respectively. The area under

Percentage of secondary structure elements in recombinant αB-Crys

αB-Cry	α-Helix	β-Sheet	β-Turn	Random coil
Wild-type	11.43	35.19	16.50	36.72
Mutant	13.89	30.29	16.38	39.42

the aggregation curves reflects the combined action of the three above-mentioned parameters, which are normally used for quantification of chaperone activity. The values of $(1 - Ar/Ar_0)$ varied between 0 and 1. In the absence of chaperone, when the value of (Ar/Ar_0) is 1, the percentage of protection is zero. In the presence of a perfect chaperone, when the area under the aggregation curve (Ar) is zero, the protection will approach 100%.

In this study, to characterize chaperone activity of wild-type and mutant α-Cry, the test systems based on DTT-induced aggregation of insulin and thermally induced aggregation of γ-Cry were applied (Fig. 3). The analysis was done based on the changes in optical density at 360 nm, which was registered for 30 and 60 min in the chemical and thermally induced aggregation systems, respectively.

The aggregation progress of client proteins as a function of time is indicated in Fig. 3 (a, b) (for insulin) and Fig. 3c (for γ-Cry). The percentages of protection achieved by the chaperones in DTT-induced aggregation of insulin and in the thermally induced aggregation of γ-Cry (native molecular partner of lens α-Cry) are shown in Fig. 3, d and e, respectively. The data in Fig. 3 suggest that the mutant protein has stronger chaperone activity than the wild-type protein counterpart. The higher chaperone activity of mutant αB-Cry can be explained by its partial resistance against heat-induced self-aggregation, as indicated in Fig. 4.

Effect of thermal stress on structure and aggregation of wild-type and R12C mutant αB-Crys. As a major cause of visual impairment worldwide, cataract is the opacification of the eye lens characterized by formation of light-scattering protein aggregates in the lens and loss of vision [5]. In this study, the conformational instability and aggregation propensity of wild-type and mutant αB-Cry were investigated under thermal stress. Both wild-type

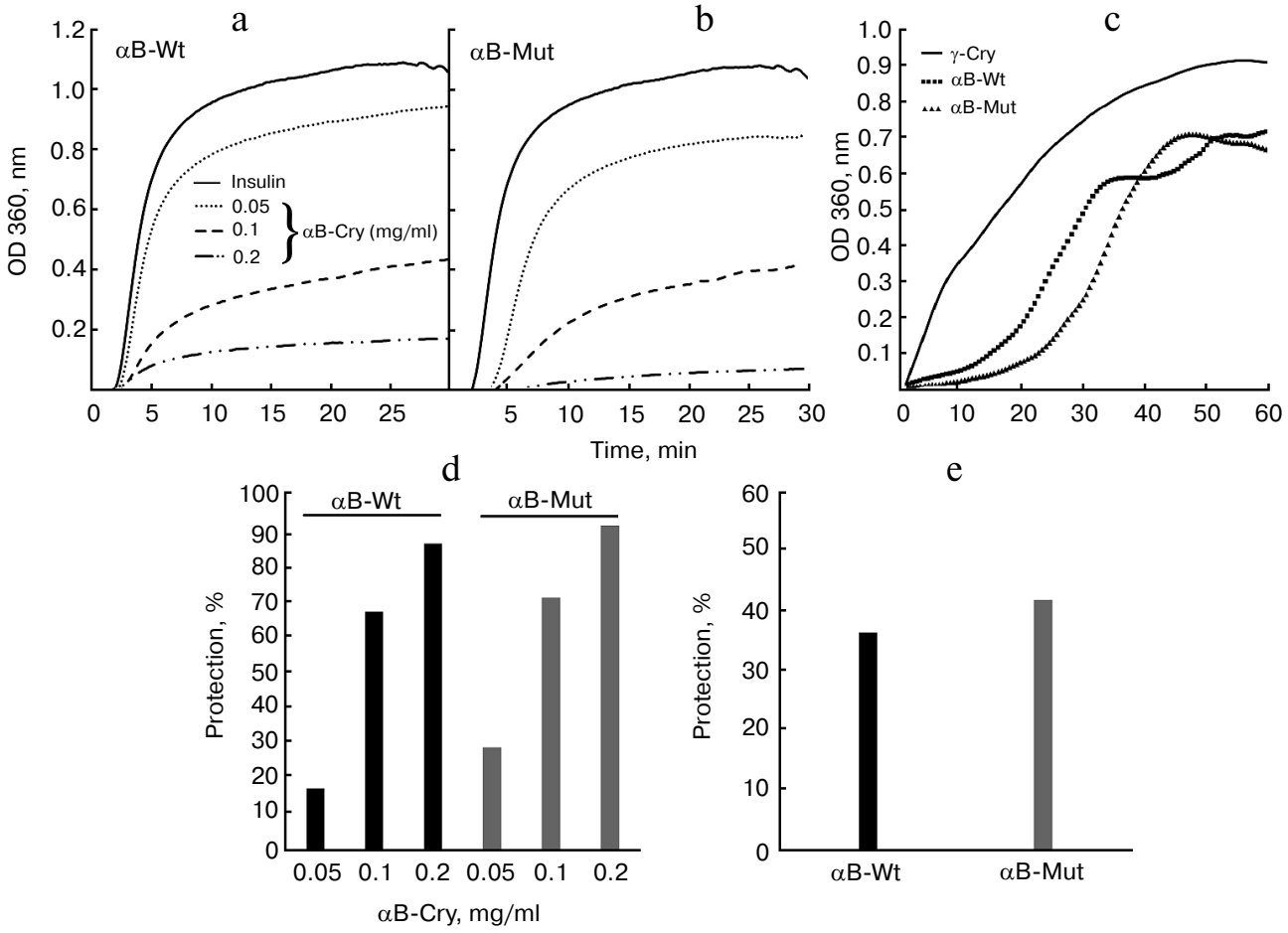

Fig. 3. Comparison of chaperone activity of wild-type and R12C mutant αB-Cry. The chaperone activity was assessed under both chemically and thermally induced aggregation. In the chemically induced aggregation system, insulin (0.3 mg/ml) was used as target protein, and aggregation was induced in the presence of 20 mM DTT at 37°C. a, b) Chaperone action of wild-type and mutant αB-Cry in this system; c) chaperone activity of these proteins in heat-induced aggregation system at 60°C for 60 min, while γ-Cry (0.3 mg/ml) was used as the target protein. These experiments were done in buffer C. d, e) The percentages of protection achieved by these chaperones in the DTT-induced aggregation of insulin and in the thermally induced aggregation of γ-Cry, respectively.

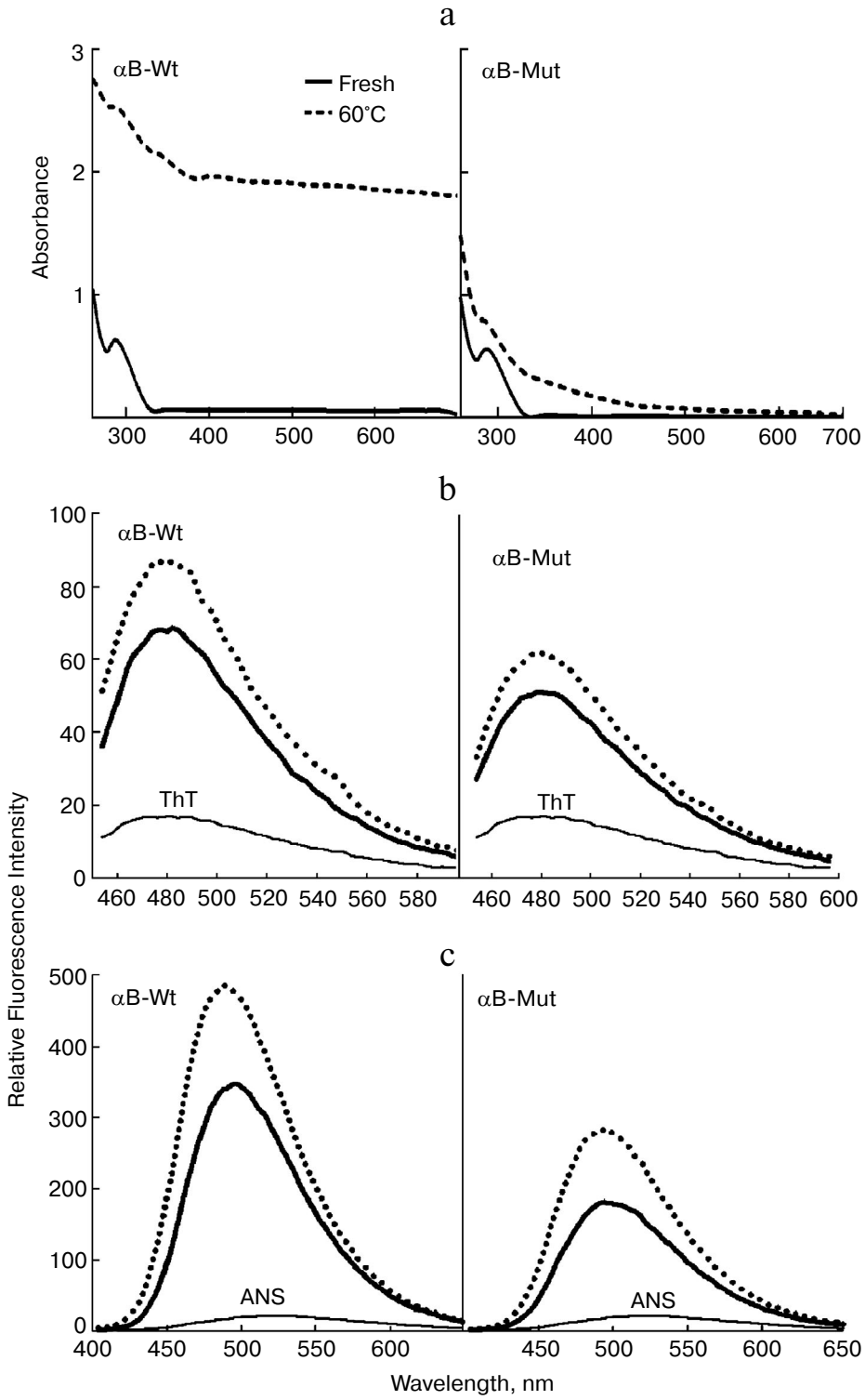

Fig. 4. Aggregation and fluorescence analysis of wild-type and mutant αB-Crys after treatment with thermal stress. a) Protein samples (1 mg/ml) were incubated at 60°C for 2 h in buffer C. Then the samples were diluted in the same buffer to final concentration 0.5 mg/ml. After that, their UV-Vis absorption spectra were recorded in the wavelength range 200-700 nm. The increment of absorbance in the visible region is indication of protein aggregation. b) Protein samples (0.15 mg/ml) were subjected to ThT fluorescence study to evaluate possible formation of ordered aggregate entities. The ThT fluorescence spectra were taken between 450-600 nm at excitation wavelength 440 nm. c) Protein samples (1 mg/ml) were heated at 60°C for 2 h. Then they were diluted to 0.15 mg/ml and subjected to ANS fluorescence analysis. For ANS fluorescence studies, the protein samples were excited at 365 nm, and the corresponding spectra were collected in the indicated ranges.

and mutant protein (1 mg/ml) were incubated at 60°C for 2 h. Then, the protein samples were diluted to a final concentration of 0.5 mg/ml and their absorption spectra were measured in the range 200-700 nm.

As shown in Fig. 4a, the significant increment in the visible region of absorption spectrum of wild-type protein is an indication of extensive protein aggregation under thermal stress. In addition, the R12C mutant that was subjected to similar thermal stress appreciably resisted aggregation. Additionally, the protein samples were assessed by ThT fluorescence analysis. As shown in Fig. 4b, both recombinant proteins demonstrate an increment of fluorescence emission in comparison with their non-heated protein counterparts. This dye has been used to diagnose the existence of protein amyloid fibrils [28]. Therefore, the enhancement of ThT fluorescence emission suggests the possible formation of amyloid fibril entity during incubation of the recombinant proteins under thermal stress. Figure 4c indicates ANS fluorescence emission of these proteins. Both proteins indicate enhancement in ANS fluorescence intensity, suggesting that heat induces exposure to the solvent of hydrophobic patches in these proteins. The exposure of hydrophobic patches of these proteins because of heat stress can further explain their heat-induced aggregation propensity as discussed above.

Effect of calcium on structure and chaperone activity of wild-type and mutant R12C. Calcium-induced activation of calpains has been implicated in the processing of lens crystallins during lens maturation and cataract formation [5, 10]. Moreover, a significant elevation of calcium level has been reported in both human and experimental animal cataracts, and this elevation has been implicated to contribute to cataractogenesis [4, 11, 16]. In this study, αB-Cry was incubated with different concentrations of calcium chloride (0, 1, and 5 mM) for one week at 37°C. At the end, the protein samples were individually diluted in the same buffer and used for structural investigation by fluorescence spectroscopy (Fig. 5).

The Trp fluorescence emission spectra of both wild-type and mutant protein indicate a gradual reduction with further increase of calcium concentration (Fig. 5a). These results suggest that calcium induces protein structural changes that are accompanied with the movement

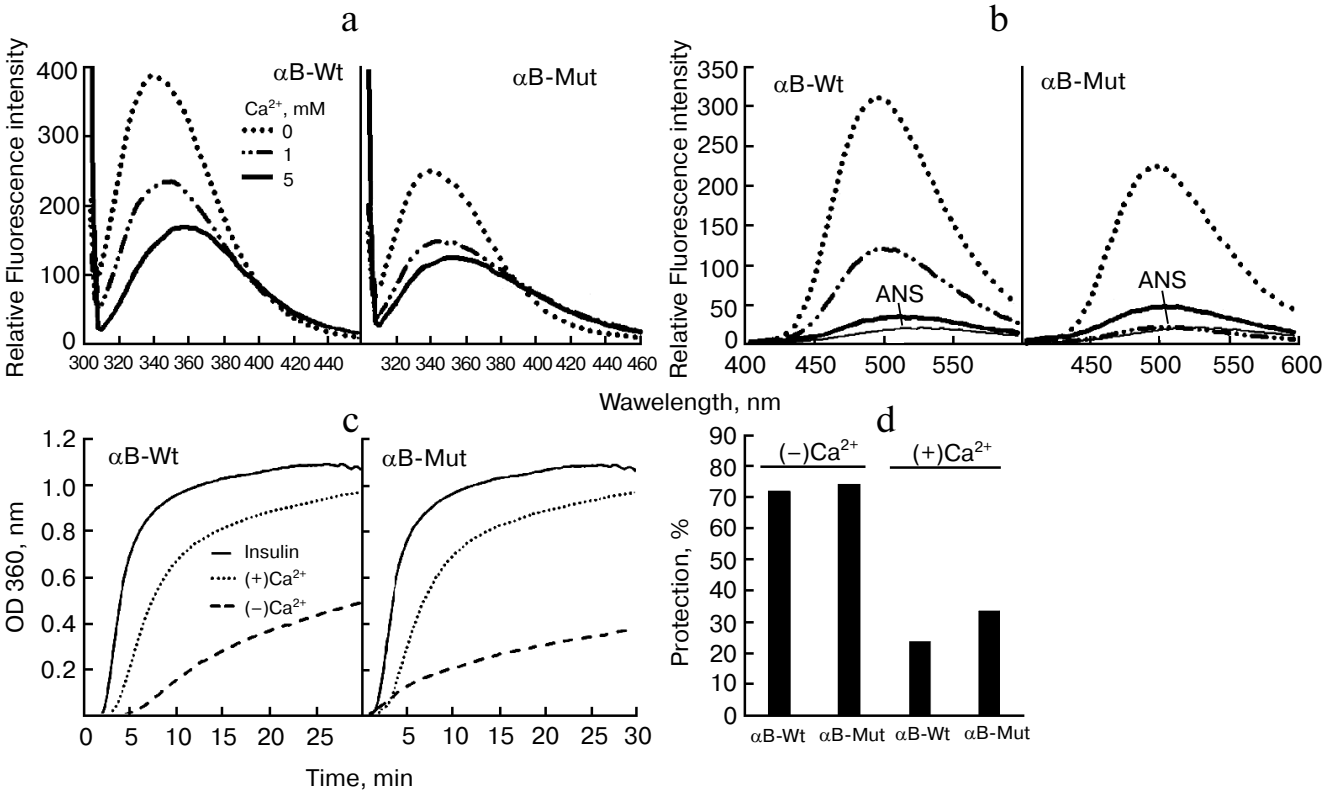

Fig. 5. Structural analysis and chaperone activity assessment of wild-type and R12C αB-Crys in the presence of calcium ion. The recombinant αB-Crys were incubated with different concentrations of calcium ions (0, 1, and 5 mM) for one week at 37°C. At the end of the incubation, the protein samples were diluted and used for structural investigation by fluorescence spectroscopy in buffer C at 25°C. a) Trp fluorescence measurements were done with protein samples (0.15 mg/ml) excited at 295 nm, and emission spectra were collected in the range 300-500 nm. b) Protein samples (0.15 mg/ml) were incubated with ANS (100 μM) for 30 min and then excited at 365 nm, while their emission spectra were recorded between 400 and 600 nm. c) Chaperone activity was assessed in buffer C in the presence of 5 mM calcium. Insulin (0.3 mg/ml) was used as the target protein, while the induction of insulin aggregation was followed in the presence of 20 mM DTT. d) Chaperone activity is expressed in terms of percentage of protection according to Eq. (2).

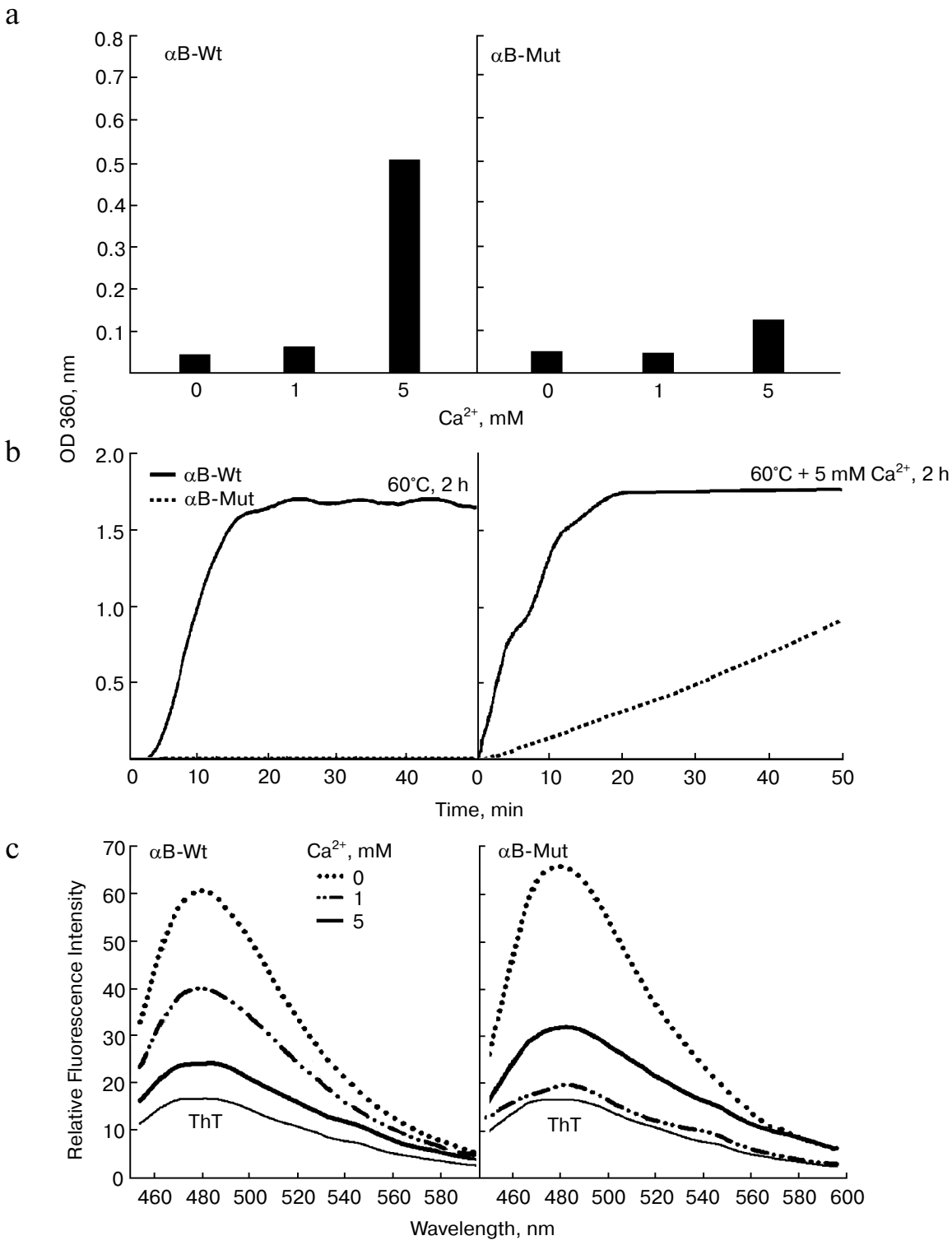

Fig. 6. Aggregation and ThT fluorescence analysis of wild-type and R12C mutant αB-Crys in the presence of calcium. a) Both wild-type and mutant αB-Crys (0.5 mg/ml) were incubated with calcium ion at 37°C for one week in buffer C. The protein samples were diluted in the same buffer to final concentration 0.15 mg/ml. Then their UV-Vis absorption spectra were collected in the wavelength range 200-700 nm. The increment of absorbance at 360 nm was used as indication of protein aggregation. b) Aggregation of recombinant αB-Crys was evaluated in kinetic fashion under thermal stress and thermal stress with 5 mM calcium ion. While the concentration of protein samples was fixed at 0.5 mg/ml, the experiments were done in buffer C. c) Protein samples (0.15 mg/ml) were subjected to ThT fluorescence study to evaluate formation of ordered aggregate entities. The ThT fluorescence spectra were taken between 450-600 nm with excitation wavelength 440 nm.

of Trp residues to a polar environment. In addition, to investigate the impact of calcium on hydrophobic surface of these proteins, ANS fluorescence was studied. As shown in Fig. 5b, significant reductions in ANS fluorescence intensity of both wild-type and mutant proteins were observed. The results clearly indicate that the structural variations induced by calcium result in significant reduction of hydrophobic surfaces in these proteins. Homeostasis of intracellular calcium is crucial for lens cytoarchitecture and transparency [5, 16]. In addition, additional to the specific role of calcium in the activation of lenticular calpains, the structural alteration of α-Cry in the presence of this metal ion is highly significant in the development of lens opacification and cataract disorders (scheme). As the major molecular chaperone of eye lens, α-Cry functions to maintain transparency of lenticular tissue [4, 10, 11]. In addition to the chaperone activity, αB-Cry plays a role in several cellular processes, such as signal transduction, protein degradation, stabilization of cytoskeletal structures, and apoptosis [40]. Moreover, mutations in the αB-Cry gene can have detrimental effects leading to pathologies such as cataract and cardiomyopathy [19]. In this study, the chaperone activity of both wild-type and mutant αB-Cry were assessed in the absence and presence of 5 mM calcium. The chaperone activity was measured in a chemical-induced aggregation system, as insulin was the target protein (Fig. 5, c and d). As shown in these figures, calcium reduces chaperone activity of both recombinant proteins to a significant level. The reduction in chaperone activity can be explained by the lessening of surface hydrophobicity of these proteins in the presence of calcium, and the level of hydrophobic surfaces is known to be a major determinant of chaperone activity in α-Cry (Fig. 5b). In fact, the entropically driven hydrophobic contacts between α-Cry-accessible hydrophobic surfaces and newly exposed hydrophobic sites of unfolding substrates is one of the major forces implicated in the mechanistic action of this protein. Overall, the changes in structure and chaperone activity of these recombinant proteins may offer molecular insight into the mechanism of lens opacification.

Effect of calcium on aggregation of wild-type and R12C mutant αB-Crys. The structural transformations and aggregation of α-Cry underlie cataract formation and cause clouding of the eye lens, leading to partial or total loss of vision [24, 25]. On the other hand, calcium as a cataractogenic metal ion has been indicated to induce aggregation of α-Cry [11, 16]. To assess the impact of calcium ion on aggregation of wild-type and mutant αB-Cry, the recombinant proteins (1 mg/ml) were incubated with different concentrations of this metal ion for one week at 37°C. At the end of the incubation, the protein samples were diluted in the same buffer to final concentration 0.5 mg/ml and their UV-Vis absorption spectra were measured in the range 200-700 nm (Fig. 6).

The increment of absorbance at 280 nm is an important indication of protein unfolding, while the enhancement of absorbance in the wavelength range above 320 nm indicates protein aggregation [11, 24]. As shown in Fig. 6a, at calcium concentration 5 mM, these recombinant proteins display extensive unfolding and aggregation. In addition, the extent of aggregation was significantly higher in the case of wild-type protein compared to the mutant protein counterpart. This finding is in good agreement with the data of thermal-induced aggregation of these proteins as indicated in Fig. 4a. Additionally, the combined effect of both thermal stress (60°C) and calcium (5 mM) on aggregation of these proteins was evaluated in kinetic fashion (Fig. 6b). As shown in this figure, under thermal stress and in the absence of calcium, the increment of optical density at 360 nm as a function of time indicates aggregation of the wild-type protein. Under similar condition, the mutant protein counterpart resists aggregation. However, under thermal stress and in the presence of 5 mM calcium, the aggregation of wild-type protein lacks any lag time, showing strong propensity of this protein for aggregation. According to the slope of aggregation curves in the initial stages, it can be suggested that the mutant protein demonstrates significantly lower aggregation propensity than the wild-type protein counterpart. The significant resistance of R12C mutant αB-Cry against aggregation under either thermal stress or in the presence of calcium ions provides an important indication explaining the non-cataractogenic nature of this mutation compared to the same mutation in αA-Cry, which is linked to development of cataract diseases. In addition, in this study, the proteins samples were further analyzed by ThT fluorescence study (Fig. 6c). As mentioned above, the ThT fluorescence probe has been frequently used to diagnose the presence of protein amyloid fiber. As shown in Fig. 6c, the intensity of ThT emission of the protein samples incubated with calcium was significantly lower than the protein sample incubated without this metal ion. These results suggest that under the experimental condition calcium did not induce the formation of ordered aggregation in the recombinant proteins. Cataract, the leading cause of blindness worldwide, is caused by protein aggregation within the protected lens environment. The attenuation of chaperone activity and aggregation of αB-Cry in the presence of calcium ion can be of significance to further understand the molecular details of different factors that are involved in the pathogenesis of cataract disorders. Moreover, αB-Cry has been detected in various non-ocular tissues, and its upregulation has been indicated before in pathological conditions such as neurodegenerative diseases, cancers, diabetes, retinal diseases, cataracts, ischemia/reperfusion, and aging [8, 9]. Therefore, the deleterious impacts of calcium ion on αB-Cry are not limited to lenticular tissues and/or ocular disorders.

Gel mobility shift analysis of αB-Cry oligomerization. SDS-PAGE under reducing and non-reducing conditions has been frequently used for determination of pro-

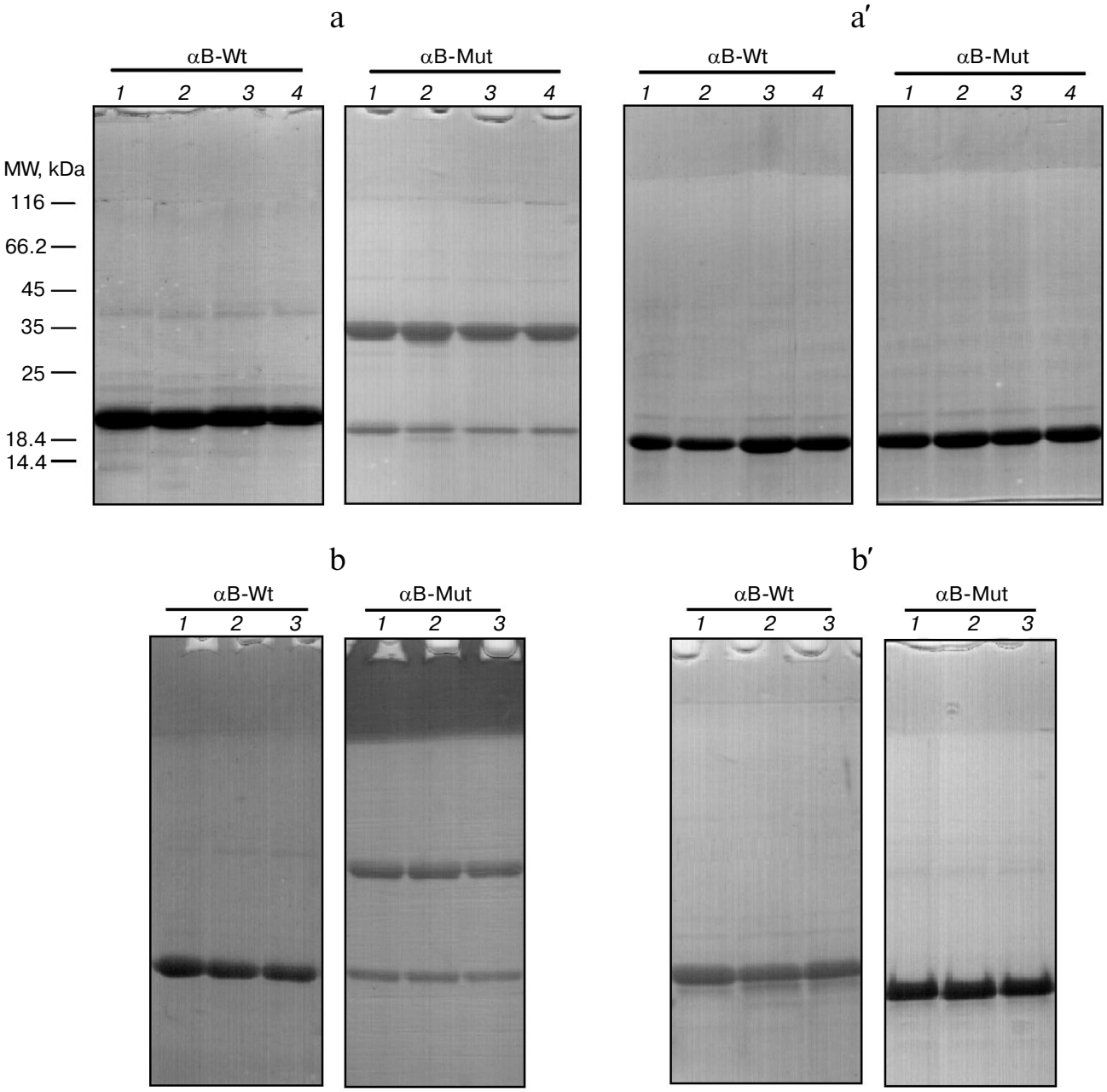

Fig. 7. Gel mobility shift analysis of recombinant αB-Crys after heat treatment and in the presence of calcium. Protein samples (1 mg/ml) were individually incubated under thermal stress (60°C) or thermal stress with calcium ion for 2 h. a, a′) Mobility shift analysis of recombinant proteins are indicated after incubation with the thermal stress. Lanes *1-4*, respectively, show the incubation of these proteins under stress condition for 0, 30, 60, and 120 min. b, b′) Results of mobility shift analysis of protein samples that were incubated under thermal stress and in the presence of 5 mM calcium. Lanes *1-3*, respectively, show the incubation of these proteins with different concentrations of calcium ions as 0, 1, and 5 mM. At the end of the incubations, an aliquot (12 μg) of each protein sample was taken and subjected to SDS-PAGE analysis (12% gel), under non-reducing (a, b) and reducing (a′, b′) conditions. Protein bands were visualized by CBB staining.

tein oligomerization state [41]. The αB-Cry samples subjected to the thermal stress (60°C) for different incubation times (0, 30, 60, and 120 min) were individually withdrawn and analyzed by SDS-PAGE under non-reducing (a) and reducing (a′) conditions (Fig. 7a). As shown in this figure, the R12C mutant protein shows intrinsic ability for dimerization due to its newly incorporated Cys residue. Thermal stress results in slight reduction of the intensity of the band corresponding to the monomeric form of this protein. Applying reducing condition, the bands corresponding to dimeric the form of the mutant protein completely disappeared, suggesting involvement of disulfide bridge-mediated dimerization of this protein. The role of disulfide cross-linking among lens crystallins

has been already indicated in the pathogenesis of cataract disorder [42].

Therefore, the intrinsic ability of this protein for disulfide bridge-mediated oligomerization may explain the pathomechanism of cataract diseases. As the protein samples were incubated with different concentrations of calcium ion (0, 1, and 5 mM) under thermal stress (60°C) for 2 h, the electrophoretic mobility of the protein bands was roughly similar to the results of a corresponding experiment in the absence of calcium ion (Fig. 7b). In addition, the protein samples were incubated with different concentrations of calcium at 37°C for 24 h. At the end of the incubations, as the mobility shift analysis was performed on SDS-PAGE gel, similar results were obtained (see figure in Supplement to this paper on the site of the journal (http://protein.bio.msu.ru/biokhimiya) and on Springer site (Link.springer.com)).

While αB-Cry is expressed in lenticular and several other tissues, its upregulation has been already reported in different pathological states. In this study both wild-type and R12C mutant αB-Crys were subjected to thermal stress and also treated with calcium, which is known as an important cataractogenic element. The chaperone activity and aggregation propensity of these proteins were investigated in a comparative manner. These recombinant proteins demonstrate dissimilar structures. Compared to the wild-type αB-Cry, the mutant protein counterpart significantly resists thermal and calcium-induced aggregation. Additionally, upon mutation this protein indicated a slight improvement in its chaperone activity. These results may explain to some extent the non-cataractogenic nature of R12C mutation in αB-Cry. Additionally, in the presence of calcium ion, the chaperone activity of these recombinant proteins was attenuated to a significant level. In addition, the R12C mutant protein indicates significant propensity for disulfide bridge-mediated self-dimerization. Overall, the results of this study offer further molecular insight into the pathomechanism of different factors that contribute to development of cataract diseases.

We thank the financial support of the Iran National Science Foundation (INSF), Grant No. 92001695. In addition, the financial support of research councils of Shiraz University is gratefully acknowledged.

REFERENCES

1. Laganowsky, A., Benesch, J. L., Landau, M., Ding, L., Sawaya, M. R., Cascio, D., Huang, Q., Robinson, C. V., Horwitz, J., and Eisenberg, D. (2010) Crystal structures of truncated alpha A and alpha B crystallins reveal structural mechanisms of polydispersity important for eye lens function, *Protein Sci.*, **19**, 1031-1043.
2. Horwitz, J. (2003) Alpha-crystallin, *Invest. Exp. Eye Res.*, **76**, 10-22.
3. Van Boekel, M. A., De Lange, F., De Grip, W. J., and De Jong, W. W. (1999) Eye lens αA-and αB-crystallin: complex stability versus chaperone-like activity, *Biochim. Biophys. Acta*, **1434**, 114-123.
4. Clark, J. I., and Muchowski, P. J. (2000) Small heat-shock proteins and their potential role in human disease, *Curr. Opin. Struct. Biol.*, **10**, 52-59.
5. Jedziniak, J. A., Kinoshita, J. H., Yates, E. M., Hocker, L. O., and Benedek, G. B. (1972) Calcium-induced aggregation of bovine lens alpha crystallins, *Invest. Ophthalmol. Vis. Sci.*, **11**, 905-915.
6. Testa, M., Fiore, C., Bocci, N., and Calabro, S. (1968) Effect of the oxidation of sulfhydryl groups on lens proteins, *Exp. Eye Res.*, **7**, 276-290.
7. Ganadu, M. L., Aru, M., Mura, G. M., Coi, A., Mlynarz, P., and Kozlowski, H. (2004) Effects of divalent metal ions on the αB-crystallin chaperone-like activity: spectroscopic evidence for a complex between copper (II) and protein, *J. Inorg. Biochem.*, **98**, 1103-1109.
8. Del Valle, L. J., Escribano, C., Perez, J. J., and Garriga, P. (2002) Calcium-induced decrease of the thermal stability and chaperone activity of α-crystallin, *Biochim. Biophys. Acta*, **1601**, 100-109.
9. Moyano, J. V., Evans, J. R., Chen, F., Lu, M., Werner, M. E., Yehiely, F., Diaz, L. K., Turbin, D., Karaka, G., Weily, E., Nielsen, T. O., Perou, C. M., and Cryns, V. L. (2006) αB-Crystallin is a novel oncoprotein that predicts poor clinical outcome in breast cancer, *J. Clin. Invest.*, **116**, 261-270.
10. Chebotareva, N. A., Eronina, T. B., Sluchanko, N. N., and Kurganov, B. I. (2015) Effect of Ca^{2+} and Mg^{2+} ions on oligomeric state and chaperone-like activity of αB-crystallin in crowded media, *Int. J. Biol. Macromol.*, **76**, 86-93.
11. Hawse, J. R., Cumming, J. R., Oppermann, B., Sheets, N. L., Reddy, V. N., and Kantorow, M. (2003) Activation of metallothioneins and α-crystallin/sHSPs in human lens epithelial cells by specific metals and the metal content of aging clear human lenses, *Invest. Ophthalmol. Vis. Sci.*, **44**, 672-679.
12. Hightower, K. R., Leverenz, V., and Reddy, V. N. (1980) Calcium transport in the lens, *Invest. Ophthalmol. Vis. Sci.*, **19**, 1059-1066.
13. Borchman, D., Delamere, N. A., and Paterson, C. A. (1988) Ca-ATPase activity in the rabbit and bovine lens, *Invest. Ophthalmol. Vis. Sci.*, **29**, 982-987.
14. Tang, D., Borchman, D., Yappert, M. C., Vrensen, G. F., and Rasi, V. (2003) Influence of age, diabetes, and cataract on calcium, lipid–calcium, and protein–calcium relationships in human lenses, *Invest. Ophthalmol. Vis. Sci.*, **44**, 2059-2066.
15. Biswas, S., Harris, F., Singh, J., and Phoenix, D. (2004) Role of calpains in diabetes mellitus-induced cataractogenesis: a mini review, *Mol. Cell. Biochem.*, **261**, 151-159.
16. Mainz, A., Bardiaux, B., Kupller, F., Multhaup, G., Felli, I. C., Pierattelli, R., and Reif, B. (2012) Structural and mechanistic implications of metal binding in the small heat-shock protein αB-crystallin, *J. Biol. Chem.*, **287**, 1128-1138.
17. Brookes, P. S., Yoon, Y., Robotham, J. L., Anders, M. W., and Sheu, S. S. (2004) Calcium, ATP, and ROS: a mitochondrial love–hate triangle, *Am. J. Physiol. Cell Physiol.*, **287**, 817-833.

18. Nagaraj, R. H., Panda, A. K., Santhoshkumar, S., Santhoshkumar, P., Pasupuleti, N., Wang, B., and Biswas, A. (2012) Hydroimidazolone modification of the conserved Arg12 in small heat shock proteins: studies on the structure and chaperone function using mutant mimics, *PloS One*, **7**, e30257.
19. Plater, M. L., Goode, D., and Cerabbe, M. J. (1996) Effects of site-directed mutations on the chaperone-like activity of αB-crystallin, *J. Biol. Chem.*, **271**, 28558-28566.
20. Ahmad, M. F., Raman, B., Ramakrishna, T., and Rao, Ch. M. (2008) Effect of phosphorylation on αB-crystallin: differences in stability, subunit exchange and chaperone activity of homo and mixed oligomers of αB-crystallin and its phosphorylation-mimicking mutant, *J. Mol. Biol.*, **375**, 1040-1051.
21. Boelens, W. C., Croes, Y., De Ruwe, M., De Reu, L., and De Jong, W. W. (1998) Negative charges in the *C*-terminal domain stabilize the αB-crystallin complex, *J. Biol. Chem.*, **273**, 28085-28090.
22. Biswas, A., and Das, K. P. (2004) Role of ATP on the interaction of α-crystallin with its substrates and its implications for the molecular chaperone function, *J. Biol. Chem.*, **279**, 42648-42657.
23. Sun, T. X., Das, B. K., and Liang, J. J. (1997) Conformational and functional differences between recombinant human lens αA- and αB-crystallin, *J. Biol. Chem.*, **272**, 6220-6225.
24. Yousefi, R., Khazaei, S., and Moosavi-Movahedi, A. A. (2013) Effect of homocysteinylation on structure, chaperone activity and fibrillation propensity of lens alpha-crystallin, *Protein Pept. Lett.*, **20**, 932-941.
25. Khalili-Hezarjaribi, H., Yousefi, R., and Moosavi-Movahedi, A. A. (2012) Effect of temperature and ionic strength on structure and chaperone activity of glycated and non-glycated alpha-crystallin, *Protein Pept. Lett.*, **19**, 450-457.
26. Bradford, M. M. (1976) A rapid and sensitive method for the quantitation of microgram quantities of protein utilizing the principle of protein–dye binding, *Anal. Biochem.*, **72**, 248-254.
27. Ghahramani, M., Yousefi, R., Khoshaman, K., and Alavianmehr, M. M. (2015) The impact of calcium ion on structure and aggregation propensity of peroxynitrite-modified lens crystallins: new insights into the pathogenesis of cataract disorders, *Colloids Surf. B Biointerfaces*, **125**, 170-180.
28. Paoli, P., Sbrana, F., Tiribilli, B., Caselli, A., Pantera, B., Cirri, P., De Donatis, A., Formigli, L., Nosi, D., Manao, G., Camici, G., and Ramponi, G. (2010) Protein N-homocysteinylation induces the formation of toxic amyloid-like protofibrils, *J. Mol. Biol.*, **400**, 889-907.
29. Kelly, S. M., Jess, T. J., and Price, N. C. (2005) How to study proteins by circular dichroism, *Biochim. Biophys. Acta*, **1751**, 119-139.
30. Liang, J., and Rossi, M. (1989) Near-ultraviolet circular dichroism of bovine high molecular weight α-crystallin, *Invest. Ophthalmol. Vis. Sci.*, **30**, 2065-2068.
31. Bohm, G., Muhr, R., and Jaenicke, R. (1992) Quantitative analysis of protein far UV circular dichroism spectra by neural networks, *Protein Eng.*, **5**, 191-195.
32. Liang, J. J., Sun, T. X., and Akhtar, N. J. (2000) Heat-induced conformational change of human lens recombinant αA- and αB-crystallins, *Mol. Vis.*, **6**, 10-14.
33. Schagger, H. (2006) Tricine–SDS-PAGE, *Nat. Protoc.*, **1**, 16-22.
34. Berengian, A. R., Bova, M. P., and Mchaourab, H. S. (1997) Structure and function of the conserved domain in αA-crystallin. Site-directed spin labeling identifies a β-strand located near a subunit interface, *Biochemistry*, **36**, 9951-9957.
35. Litt, M., Kramer, P., LaMorticella, D. M., Murphey, W., Lovrien, E. W., and Weleber, R. G. (1998) Autosomal dominant congenital cataract associated with a missense mutation in the human alpha crystallin gene CRYAA, *Hum. Mol. Genet.*, **7**, 471-474.
36. Devi, R. R., Yao, W., Vijayalakshmi, P., Sergeev, Y. V., Sundaresan, P., and Hejtmancik, J. F. (2008) Crystallin gene mutations in Indian families with inherited pediatric cataract, *Mol. Vis.*, **14**, 1157-1170.
37. Biswas, A., Miller, A., Oya-Ito, T., Santhoshkumar, P., Bhat, M., and Nagaraj, R. H. (2006) Effect of site-directed mutagenesis of methylglyoxal-modifiable arginine residues on the structure and chaperone function of human RA-crystallin, *Biochemistry*, **45**, 4569-4577.
38. Kurganov, B. I. (2002) Kinetics of protein aggregation. Quantitative estimation of the chaperone-like activity in test-systems based on suppression of protein aggregation, *Biochemistry (Moscow)*, **67**, 409-422.
39. Kurganov, B. I. (2013) Antiaggregation activity of chaperones and its quantification, *Biochemistry (Moscow)*, **78**, 1554-1566.
40. Mao, Y. W., Liu, J. P., Xiang, H., and Li, D. W. (2004) Human αA- and αB-crystallins bind to Bax and Bcl-XS to sequester their translocation during staurosporine induced apoptosis, *Cell Death Differ.*, **11**, 512-526.
41. Cumming, R. C., Andon, N. L., Haynes, P. A., Park, M., Fischer, W. H., and Schubert, D. (2004) Protein disulfide bond formation in the cytoplasm during oxidative stress, *J. Biol. Chem.*, **279**, 21749-21758.
42. Yu, N. T., De Nagel, D. C., Pruett, P. L., and Kuck, J. F. (1985) Disulfide bond formation in the eye lens, *Proc. Natl. Acad. Sci. USA*, **82**, 7965-7968.